Biophysical Chemistry, 44 (1992) 151–161
Elsevier Science Publishers B.V., Amsterdam

BIOCHE 01685

Enhanced biopotency of synthetic C3a analogues by membrane binding. A fluorescence anisotropy decay study [1]

M. Federwisch [a], M. Casaretto [b], R. Gerardy-Schahn [c], D. Bitter-Suermann [c] and A. Wollmer [a]

[a] *Institut für Biochemie, Rheinisch-Westfälische Technische Hochschule Aachen, Klinikum, Pauwelsstr. 30, D-5100 Aachen (Germany)*
[b] *Deutsches Wollforschungsinstitut Veltmanplatz 8, D-5100 Aachen (Germany)*
[c] *Institut für Medizinische Mikrobiologie, Medizinische Hochschule Hannover, D-3000 Hannover 61 (Germany)*

Abstract

The biological activity of oligopeptide analogues of C3a is markedly increased by N-terminal attachment of a hydrophobic group as, for instance, 9-fluorenylmethoxycarbonyl (Fmoc), either direct or via a flexible 6-aminohexanoyl (Ahx) spacer. This study presents evidence from fluorescence anisotropy decay measurements that the hydrophobic appendix mediates non-specific binding of the synthetic peptide analogues to phospholipid vesicles. According to quantitative considerations no alternative or additional rate-enhancing mechanisms other than surface diffusion are required to account for the gain in biopotency.

Keywords: C3a analogues; Phospholipid vesicles; Biopotency enhancement by membrane binding; Fmoc as membrane anchor and fluorophore; Fluorescence anisotropy decay for monitoring binding

1. Introduction

The anaphylatoxin C3a is an important mediator of inflammation. It influences immune regulatory responses, contracts smooth muscle tissue, and causes serotonin and ATP release from and aggregration of platelets [1–3]. The protein consists of 77 amino acids, but the minimal sequence that exhibits biological activity at all is the C-terminal pentapeptide LGLAR or, in combination with Fmoc–Ahx, even the tripeptide LAR [4]. To maximize the biological activity of synthetic C3a analogues we designed and synthesized a series of peptide derivatives with a length between 5 and 21 amino acids and N-terminal non-peptidic extensions. The peptide moiety may correspond to the "message" and the non-peptidic part to the "address" segment in the concept of Gremlich et al. [5]. Message and address segment can be separated by a spacer [6].

Peptides carrying the Fmoc group at their N-terminus were found to exhibit increased biological activity. They were also shown to bind to glycodeoxycholate (GDC) micelles. It was therefore hypothesized that the observed increase in

Correspondence to: Dr. A. Wollmer, Institut für Biochemie, Rheinisch-Westfälische Technische Hochschule Aachen, Klinikum, Pauwelsstr. 30, D-5100 Aachen (Germany) Tel. (0241) 8088850, fax: (0241) 8088851.

[1] From the thesis of M. Federwisch.

biopotency is due to an increase in two-dimensional concentration by non-specific binding to the plasma membrane [6]. Hence, the non-peptidic extension is believed to act as a membrane anchor and not to bind to an "address" site on the receptor itself.

In the study reported here this hypothesis was examined against the background of Berg's theory of surface diffusion as rate-enhancing mechanism in macromolecular association [7]. As a more adequate model for biological membranes egg yolk phosphatidylcholine vesicles [8,9] were used here instead of GDC micelles. The peptide solutions were titrated with a stable suspension of vesicles. As a novel method for monitoring binding, fluorescence anisotropy decay (FAD; for a general introduction see ref. [10]) was used with Fmoc (normally a N_α protective group in peptide synthesis) as fluorophore.

It is demonstrated that membrane binding mediated by appropriate hydrophobic N-terminal anchor groups can fully account for the increased biological activity observed with these peptides. Formation of hydrophobic or amphipathic helices is not a *conditio sine qua non* for binding and activity [11–14] as the peptides are too short and/or their circular dichroism is hardly affected.

2. Materials and methods

2.1 Peptides

The peptides were synthesized as described previously and purified by low-pressure reversed phase chromatography and ion exchange on CM cellulose at pH 4.5. They were all homogeneous in different solvent systems in HPLC and TLC. as well as in electrophoresis at pH 2.6. The amino acid analyses corresponded to the theoretical values [6,15]. Only P10 was a generous gift from Multiple Peptide Systems, San Diego, U.S.A.

All other chemicals are commercially available and were of p.a. grade. The water was prepared with a Milli-Q system (Millipore S.A., Molsheim, France).

2.2 Biological activity

The *in vitro* biopotency of the C3a analogues relative to guinea pig C3a was determined in the guinea pig platelet ATP-release assay (ARA) as described in [6].

2.3 Solutions

The peptides were dissolved in 10 m*M* Tris/HCl (Fluka, MicroSelect), pH 7.3, 100 m*M* NaCl. P1 and P2 had to be initially dissolved in dimethylformamide (DMF) whose final concentration was below 0.1%. For CD measurements NaCl was replaced by NaF for better transparency in the far UV.

2.4 Concentrations

Concentrations were determined photometrically using a Pye-Unicam PU 8800 UV/VIS spectrophotometer (Philips, Kassel, Germany). The molar extinction coefficients used here are $\epsilon(276) = 1{,}490\ M^{-1}\ cm^{-1}$ for Tyr [16], $\epsilon(281) = 5{,}690\ M^{-1}\ cm^{-1}$ for Trp [16], $\epsilon(299) = 5{,}900\ M^{-1}\ cm^{-1}$ for the Fmoc group and $\epsilon(301) = 11{,}500\ M^{-1}\ cm^{-1}$ for the Sulfmoc group. The latter two were determined by quantitative amino acid analysis. For the FAD measurements the concentrations of the peptides were adjusted to an optical density ≤ 0.1 (1 cm) at the wavelength of their excitation.

2.5 Vesicles

Single bilayer vesicles were prepared from egg yolk phosphatidylcholine (Fluka) according to Brunner et al. [17]. The excess of the sodium cholate used for dispersing the lecithin was removed by gel filtration on a Sephadex G-50 column. Background fluorescence originating in the vesicles was negligible except for P10, where traces of tryptophan had to be destroyed by *N*-bromosuccinimide (NBS) prior to the gel filtration. To determine the phospholipid concentration the lipids were hydrolysed at 150°C by sulphuric acid and hydrogen peroxide. The released inorganic phosphate was determined colorimetri-

cally by the method of Bartlett [18]. The concentration varied within ±5% from preparation to preparation.

2.6 Spectroscopy

CD measurements were carried out on an AVIV (Lakewood, NJ, U.S.A.) 62 DS CD spectrometer calibrated with a 0.1% aqueous solution of d-10-camphorsulphonic acid [19]. Further details were described earlier [20]. To determine the secondary structural composition the spectra were analysed with the CONTIN program package [21].

Corrected fluorescence spectra were recorded on a Spex Fluorolog 211 photon counting spectrofluorimeter (Spex Industries, NY, U.S.A.).

For fluorescence titration the vesicle suspension was added to the peptide solution in small aliquots. The advantage of adding vesicles to the peptide is that the fluorescence intensity remains approximately constant and self-absorption does not compromise the anisotropy. Changes in fluorescence were complete within ten minutes.

Fluorescence lifetimes and FAD were measured in the single photon counting mode with an Edinburgh Instruments Ltd. (U.K.) spectrometer, Model 199. The full width at half maximum (FWHM) of the lamp pulse from the hydrogen flashlamp was ~1.4 ns. The light was passed through a monochromator, vertically polarized by a Glan–Thompson prism, and focused on a thermostated quartz cuvette. The emission was viewed at 90° through a UV transmitting black glass filter (DUG 11, in the case of tyrosine as fluorophore) or a combination of a cut-off glass filter and a black glass filter (WG 335, BG 1 in the case of tryptophan as fluorophore, WG 320 in the case of Fmoc or Sulfmoc as fluorophore) to suppress first and second order stray light that passes the monochromator. All filters were supplied by Schott (Mainz, Germany). At least 60,000 counts were accumulated in the peak channel for the total fluorescence intensity, $S(t)$. The lamp pulse $L(t)$ was recorded with a Ludox (DuPont, Wilmington, DE, U.S.A.) suspension using incident light at the wavelength of excitation or at the maximum of fluorescence, depending on what led to a better fit. Data handling and the iterative non-linear least-squares fit of the decays were accomplished by a program supplied by Edinburgh Instruments Ltd. As an additional parameter the program offers a variable time shift between lamp pulse and decay curve. It was introduced to compensate for the photomultiplier colour effect [22] and is necessary to fit both, the total fluorescence intensity and fluorescence anisotropy decay (FAD). The quality of fit was judged by the reduced Chi-squared, χ^2, which equals one in the case of a perfect random distribution of the residuals. We also checked the random distribution of the weighted residuals [23].

All measurements were carried out at 22°C.

2.7 Theory and analysis

The rotation-free total intensity decay $S(t)$ was fitted to a sum of exponentials [24]:

$$s(t) = b_0 + \Sigma b_i \exp(-t/\tau_i), \quad i = 1, 2, \ldots, n \tag{1}$$

where b_0 represents the background caused by the dark counting noise of the instrument. b_i and τ_i are the amplitude and lifetime of the ith excited state, respectively.

With $D(t)$, the difference curve, the experimental anisotropy $R(t)$ is defined as [24]:

$$R(t) = \frac{I(t)_{vv} - gI(t)_{vh}}{I(t)_{vv} + 2gI(t)_{vh}} = \frac{D(t)}{S(t)} \tag{2}$$

where g compensates for the sensitivity of the detection system for vertically and horizontally polarized light. Two rotational modes are probably the limit which can be distinguished with current instrumentation and analytical procedures [10]:

$$r(t) = \Sigma r_i \exp(-t/\phi_i) + r_\infty, \quad i = 1, 2$$
$$r_0 = r_1 + r_2 + r_\infty \tag{3}$$

The parameters of $r(t)$ are: r_i, the anisotropies, and ϕ_i, the rotational correlation times. The limiting anisotropies are: $r(t \to 0) = r_0$, $r(t \to \infty) = r_\infty$.

Calculation of the anisotropy parameters using $D(t)$ and $s(t)$ is described in [25].

3. Results

The shortened analogues of human C3a used in this study are listed in Table 1. Their biological activity was determined relative to that of guinea pig C3a. The activity enhancing effect of the non-peptidic extension is relatively more pronounced for the shorter peptides. In order to compare the effects of different extensions for a given sequence the activity values are referred to that of the respective naked peptide (see Table 1). The enhancement factor f thus is the activity of the extended peptide divided by that of the naked peptide.

3.1 Steady state fluorescence

The spectra in Fig. 1 of the peptides P2 and P3 in pure buffer show the fluorescence of the Fmoc and the Sulfmoc group, respectively. In their presence no tyrosyl fluorescence is detectable because of its low quantum yield and energy transfer.

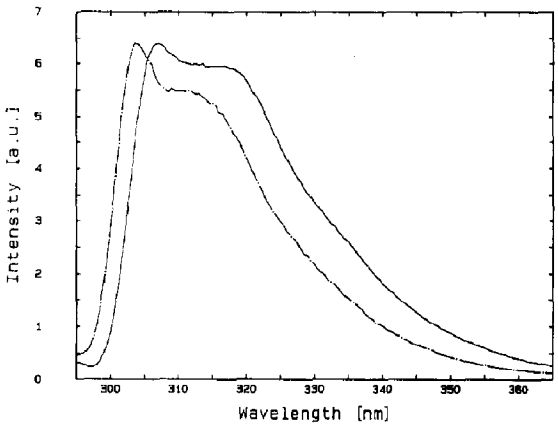

Fig. 1. Fluorescence spectra of P2 (·–·–·) and P3 (—). Excitation wavelength: 295 nm. The spectra are normalized.

Upon addition of vesicles the ratio of the intensities in the peak at 304 nm and the shoulder at 311 nm increased from 1.16 to 1.22, but no

Table 1

The effect of N-terminal hydrophobic extension on the biological activity of C3a analogues

Peptide			Biological activity			n/K_a $\times 10^3$ (M)	K_a $\times 10^{-4}$ (M^{-1})
Designation	Number of residues	Sequence	A_{C3a} (%)	Reference	f		
	6	**ALGLAR**	0.06	[6]	1	n.f.	
	6	Ahx–**ALGLAR**	0.21	[6]	3.5	n.f.	
P1	6	Fmoc–**ALGLAR**	7.6	[6]	127	0.20	5.0
P2	6	Fmoc–Ahx–**ALGLAR**	13.5	[6]	225	0.13	7.7
P3	6	Sulfmoc–Ahx–**ALGLAR**	4.2		70	b.n.d.	b.n.d.
P4	6	**Fl–ALGLAR**	n.d.			2.2 [a]	0.45
P5	5	**Rh–LGLAR**	n.d.			0.37 [a]	2.7
P6	13	**YRRGRAAALGLAR**	8.3	[6]	1	b.n.d.	b.n.d.
P7	13	Ahx–**YRRGRAAALGLAR**	36.0	[15]	4.3	b.n.d.	b.n.d.
P8	13	Fmoc–**YRRGRAAALGALR**	56.4	[6]	6.8	0.29	3.5
P9	13	Fmoc–Ahx–**YRRGRAAALGLAR**	130.0	[6]	15.7	0.17	5.9
	14	**RRQHARASHLGLAR**	4.7	[6]	1	n.f.	
P10	15	**LRRQAWRASALGLAR**	26.4		5.6	b.n.d.	b.n.d.
P11	21	**CNYITELRQRHARASHLGLAR**	9.1		1	b.n.d.	b.n.d.
P12	20	Fmoc–**NYITELRQRHARASHLGLAR**	16.1		1.8	0.26	3.9

Legend: Bold one-letter symbols of amino acid residues correspond to the native human sequence. A_{C3a}, activity relative to that of native guinea pig C3a; f, activity enhancement factor. Association constants K_a were derived from rotational correlation time titration curves. n, number of lipid molecules constituting a binding site (= 10). For further explanation see the text. Fmoc = 9-fluorenylmethoxycarbonyl; Ahx = 6-aminohexanoyl; Sulfmoc = 9-(2-sulfo)fluorenylmethoxycarbonyl; Fl = fluoresceinyl; Rh = rhodaminyl B; n.d. means not determined; b.n.d. binding not detectable; and n.f. no fluorophore.

[a] From steady state fluorescence.

wavelength shifts were observed (not shown). Because of the smallness of the effects steady state fluorescence proves inadequate for following binding to the vesicles.

3.2 Fluorescence anisotropy decay

Instead binding was monitored by FAD (for the first time to the best of our knowledge). The

Table 2

Fluorescence anisotropy decay of binding peptides as a function of the molar ratio lipid/peptide (l/c), fit with a single correlation time, ϕ. Excitation wavelength: 290 nm; bandwith: 12 nm; filter: WG 320.

(For the chemical identity of the peptides see Table 1. For the parameters listed see eq. (3) and the text)

Peptide	l/c	r_0	r_1	r_∞	ϕ (ns)	χ^2
P1	0.0	0.115	0.109	0.006	0.31	0.92
	5.8	0.142	0.126	0.016	0.45	1.63
	11.6	0.127	0.111	0.016	0.96	1.39
	17.5	0.141	0.121	0.020	0.99	1.41
	23.3	0.147	0.126	0.020	1.17	2.62
	29.1	0.157	0.135	0.021	1.24	1.78
	35.0	0.167	0.143	0.024	1.26	2.03
P2	0.0	0.121	0.119	0.002	0.15	0.94
	6.2	0.111	0.101	0.009	0.50	1.29
	12.4	0.112	0.099	0.012	0.85	1.43
	18.6	0.124	0.110	0.015	0.93	1.67
	24.8	0.127	0.112	0.014	1.22	1.81
	31.0	0.138	0.120	0.018	1.20	2.39
	37.2	0.150	0.129	0.021	1.16	1.69
P8	0.0	0.147	0.141	0.006	0.47	0.93
	6.1	0.155	0.126	0.029	0.77	1.46
	12.3	0.157	0.117	0.040	1.23	1.47
	18.4	0.163	0.115	0.047	1.77	1.85
	24.6	0.167	0.115	0.052	2.29	1.97
	30.7	0.181	0.126	0.055	2.54	2.10
	36.8	0.186	0.131	0.055	2.73	2.03
	43.0	0.187	0.133	0.054	2.96	2.24
	49.1	0.189	0.133	0.056	2.95	1.72
P9	0.0	0.118	0.118	0.0	0.35	1.04
	5.6	0.116	0.109	0.007	0.52	0.94
	11.2	0.118	0.103	0.015	0.68	1.57
	16.8	0.132	0.112	0.020	0.84	2.64
	22.4	0.144	0.127	0.017	1.19	1.40
	28.0	0.150	0.129	0.021	1.26	2.07
	33.6	0.153	0.129	0.025	1.31	1.41
P12	0.0	0.137	0.125	0.012	0.57	1.03
	5.9	0.139	0.110	0.028	1.08	1.26
	11.7	0.158	0.118	0.040	1.17	1.65
	17.6	0.160	0.114	0.046	1.60	1.61
	23.4	0.163	0.111	0.052	2.00	1.59
	29.3	0.170	0.116	0.053	2.48	1.71
	35.1	0.178	0.120	0.058	2.51	2.10
	41.0	0.178	0.123	0.055	3.32	1.95
	46.8	0.190	0.129	0.060	2.88	2.03

rotational correlation time must increase upon incorporation of the fluorophore into the membrane because of the higher viscosity there. According to this criterion the peptides can be classified into non-binding ones: P3, P6, P7, P10 and P11 and binding ones: P1, P2, P8, P9 and P12.

The group of non-binding peptides can be subdivided with respect to the fluorophores. The tyrosine containing peptides P6, P7 and P11 in the absence of vesicles had to be fitted with three decay times: $\tau_1 = 0.6–0.7$ ns, $\tau_2 = 1.7–3.0$ ns, $\tau_3 = 7.1–8.1$ ns. Upon addition of the vesicles the time-resolved fluorescence revealed only minor changes. Further non-binding peptides are P10 and P3 with tryptophan and the Sulfmoc group as fluorophore, respectively. Sulfmoc showed a single decay time, $\tau = 2.9$ ns. Data on non-binding peptides are not shown.

The fluorescence decays of all Fmoc protected binding peptides in the absence of vesicles had to be fitted with two decay times: $\tau_1 = 2.6–4.2$ ns and $\tau_2 = 5.3–7.0$ ns (data not shown) which is not unusual [26]. With P12 even a small third component had to be taken into account which caused τ_1 and τ_2 not to fall within the intervals given above. The rotational correlation time ϕ increases with increasing length of the peptides. It is, however, decreased by the flexibility introduced with the Ahx spacer (see Table 2).

Upon addition of the vesicles the width of the distribution of the decay times was narrowed: $\tau_1 = 1.4–2.0$ ns, $\tau_2 = 5.9–6.7$ ns and a third long living component with a negligible amplitude appeared (data not shown). This means that the Fmoc group independent of the peptide moiety finds itself in a more homogeneous environment. In parallel the correlation times, r_∞ and χ^2 increased (Table 2). The conclusion to be drawn is that these peptides bind to the membrane. Figures 2A and B show the decays of the total intensity and of the difference between the polarized intensities for P9 as an example.

Fitting a single correlation time yields higher χ^2. Hence, two correlation times are necessary to achieve a good fit when the peptide is bound to the membrane. For diphenylhexatriene (DPH) bound also to egg lecithin vesicles Dale et al. [26] measured: $\phi_1 = 1.4–1.9$ ns and $\phi_2 = 4.6–5.6$ ns.

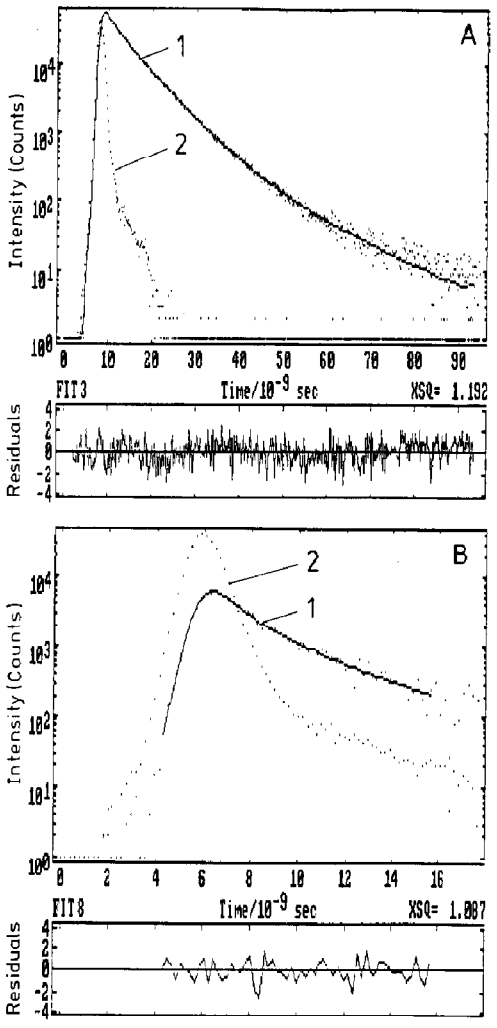

Fig. 2. Time-resolved fluorescence of P9 in the in the presence of lipid vesicles (34-fold molar excess of lipid). (A) The decay of the total fluorescence intensity $S(t)$ fitted with three lifetimes. (B) The decay of the difference $D(t)$ between the polarized fluorescence intensities fitted with two rotational correlation times. Dots: (1) measured decay: excitation wavelength: 290 nm; bandwidth: 13.6 nm; filter: WG 320. (2) lamp pulse measured at 325 nm. Continuous line: fitted decay. The residuals are shown in the lower part.

They proved that the rotation of the spherical vesicle and the lateral diffusion in its membrane are too slow to influence the measured correlation times. For the C3a peptides P1, P2, P8, P9 and P12 the correlation times were: $\phi_1 = 0.26–0.47$ ns and $\phi_2 = 2.48–5.40$ ns (data not shown).

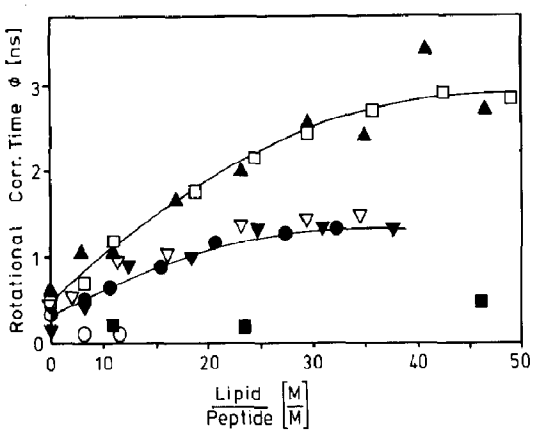

Fig. 3. Titration of the binding peptides with lipid vesicles. Rotational correlation time, ϕ (ns), as a function of the ratio of lipid concentration over constant peptide concentration ($c = 0.9 \cdot 10^{-5}$ M). The numeric values are listed in Table 2. For further explanation see the text. P1 (▽), P2 (▼), P3 (■), P6 (○), P8 (□), P9 (●) and P12 (▲).

3.3 Association constants

Figure 3 shows the titrations of the binding peptides with lipid vesicles. The (single) rotational correlation time is plotted as a function of the ratio of lipid concentration over constant peptide concentration ($c = 0.9 \cdot 10^{-5}$ M). With increasing lipid concentration the correlation time approaches a limiting value which is specific for each peptide.

The quantitative analysis of the peptide–lipid interaction was carried out according to the method Bashford et al. [27] modified by Surewicz and Epand [28]: The association constant K_a can be calculated from the slope of a plot $e - 1$ over $(e - 1)/l$:

$$e - 1 \sim \frac{n}{K_a} \cdot \frac{(e-1)}{l} \qquad (4)$$

e is the relative enhancement of the correlation time, $e = \phi(l)/\phi(l = 0)$, l the lipid concentration and n the number of lipid molecules constituting a binding site. A condition to be met is $l/n \gg c$ [27]. The total number of binding sites greatly exceeds the peptide concentration only in the final part of the titration curves. However, the limited number of reliable data points was sufficient to assess n/K_a and these values are given in Table 1. A representative value for the Fmoc peptides is 0.2 mM. It is reduced further by a factor of roughly two when the Ahx spacer is inserted.

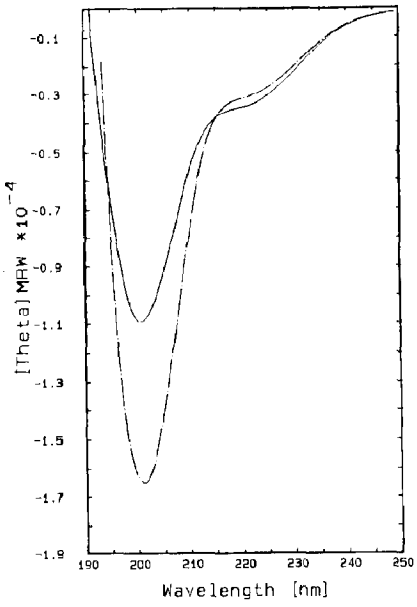

Fig. 4. Far-UV CD spectra of P11 in the absence (—) and presence (· – · – ·) of vesicles. (45-fold molar excess of lipid over peptide.)

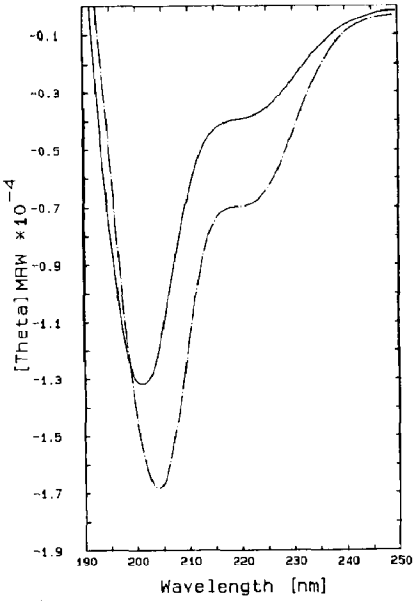

Fig. 5. Far-UV CD spectra of P12 in the absence (—) and presence (· – · – ·) of vesicles. (45-fold molar excess of lipid over peptide.)

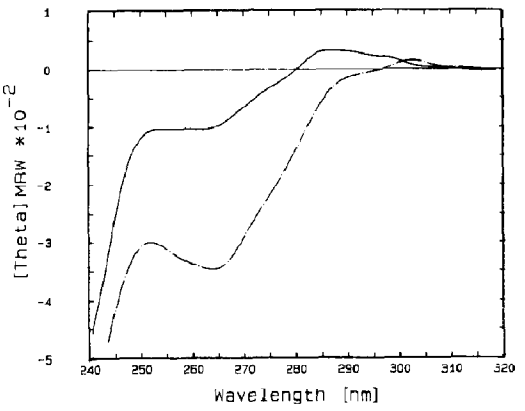

Fig. 6. Near-UV CD spectra of P12 in the absence (—) and presence (– – –) of vesicles. (45-fold molar excess of lipid over peptide.)

3.4 CD measurements

It is generally agreed that insertion of peptides into apolar/polar interfaces or into a membrane can affect their main chain conformation [5,29,30].

Figures 4 and 5 show the far-UV CD spectra of P11 and P12 in the absence and presence of vesicles. Analysis of the spectra in terms of secondary structural composition [21] results in roughly 40% irregular conformation, 25% β-structure, 20% β-turn and 15% helix, fractions that are shifted upon vesicle binding by about 5%, which is meaningless in a peptide of 20 residues. At any rate, substantial helicity formerly discussed to be an essential feature of receptor bound C3a peptides [2,3] is induced neither by vesicles nor by trifluorethanol (spectra of P6, P8 and P9 are not depicted). The increase in the near-UV CD signal of P12 upon binding to the vesicles (see Fig. 6) is indicative of its restricted mobility in the membrane.

4. Discussion

4.1 Summary of the results

The dissociation constants for the Fmoc peptides are practically independent of the peptide moiety. The Fmoc group does obviously not force the peptidic part to interact with the membrane as deducible from the CD measurements. Hence, the interaction with the membrane is solely determined by the Fmoc group which is similar to membrane probes like DPH. The further reduction of n/K_a by insertion of the Ahx spacer may result from deeper immersion into the membrane rather than from increased hydrophobicity [15].

Also hydrophobic groups like rhodamine B and fluorescein can serve as membrane anchor. Because the flashlamp intensity is insufficient above 400 nm when polarizers are used, the peptides P4 and P5 were amenable to steady state anisotropy measurements only (unpublished results). Their n/K_a's are higher than those of the Fmoc peptides (see Table 1) but still small enough that the binding occurs spontaneously.

4.2 Comparison with native C3a

Native C3a has a tendency to bind to platelet membranes as well which is presumably due to its cationic nature [31]. Gervasoni et al. [32] demonstrated that C3a binding to mast cells is mediated by heparin. Membrane binding may provide protection against carboxypeptidase N attack which would abolish activity by cleavage of the C-terminal arginine.

In the case of native C3a it remains an open question whether membrane binding implies a gain in biopotency or not. Oligopeptide analogues of C3a, however, show a correlated, sometimes spectacular, increase in membrane binding and biological activity when equipped with a N-terminal hydrophobic anchor group [4,6].

4.3 Quantitative considerations

Does non-specific binding to the membrane suffice to account for the pronounced increase in biopotency observed? As extensively discussed by Berg [7], surface diffusion may represent a rate-enhancing mechanism if two conditions are met: (1) The ligand–receptor interaction must be diffusion controlled and, (2) the effect of higher two-dimensional concentration must not be overcompensated by the reduced diffusional mobility in the membrane relative to the bulk solution.

Ad (1). Binding to the receptor is diffusion controlled if the number of receptors in the cell membrane, N, is small enough that non-specific binding to the cell surface exceeds direct specific binding to the receptor [7], i.e. if

$$N \leq \pi R/b \qquad (5)$$

A lower limit for R, the radius of a sphere representative of a platelet (an approximate cylinder of 500–2000 nm radius and 500–750 nm height) is 500 nm. The effective capture radius of the receptor, b, can be assessed from the 8 nm^2 binding area of the C5a receptor model [33] to be roughly 1.6 nm. Gerardy-Schahn et al. [34] determined 200 high- and 500 low-affinity sites per platelet. Hence, $N = 700 < 980 \leq \pi R/b$, i.e. the diffusion control condition seems to be met.

Ad (2). Despite reduced mobility in the membrane there is a net advantage of surface sliding if the constant for total non-specific binding to the cell surface is higher than $2 \cdot 10^8\ M^{-1}$ [7]. From a representative value of $2 \cdot 10^{-4}\ M$ for n/K_a (Table 1) a binding constant of $5 \cdot 10^4\ M^{-1}$ per lipid molecule is calculated assuming that 10 lipid molecules are involved in the binding of one ligand, i.e. $n = 10$. The minimum dimensions of a platelet (see above) correspond to a cellular surface of $3 \cdot 10^6$ nm^2. With 0.7 nm^2 occupied by one phosphatidylcholine molecule [35,36] $4 \cdot 10^6$ of them are exposed at the surface. Referring the binding constant for the Fmoc peptides to the cell surface yields a value of $5 \cdot 10^4\ M^{-1} \times 4 \cdot 10^6 = 2 \cdot 10^{11}\ M^{-1}$ which is higher than the limit given above. Therefore, enhanced biopotency can indeed be an effect of initial non-specific binding to the membrane.

4.4 The activity enhancement factor

The effect of Fmoc on the biopotency is relatively much more pronounced with the shorter peptides [4,6], particularly the hexapeptide (Table 1). This can be explained by their greater anchor over total molecular mass ratio and, hence, greater relative hydrophobicity [15] and by their lesser receptor affinity without anchor. The lower limit seems to be given by the shortest peptide that can trigger the receptor at all [4]. If the receptor model for C5a [33] is relevant also for C3a, there is no need for long peptides, since the receptor is a flat island in the lipid sea. On the contrary, if the Fmoc peptides exceed a certain length activity decreases again [6]. P12, for instance is only 0.3 times as active as P8. Excessive length may introduce too many degrees of freedom. After all the structure of the peptides is only poorly ordered as apparent from the CD spectra.

4.5 Where does the hydrophobic anchor group bind?

Ember et al. [37,38] proposed specific binding to a secondary binding site on the receptor because they achieved superpotency for C3a agonists which had two Trp residues attached N-terminally. As the potency varies with the length of the peptides, i.e. the distance between the essential C-terminal Arg^{77} and the N-terminal double Trp, they assumed the latter to represent a secondary hydrophobic binding site.

A hydrophobic binding site on the receptor would, however, compete with the membrane. For peptides of deficient length competition would occur further between the binding sites for their address and message segments. Despite there is no lower limit for the peptide length (see above).

Furthermore the authors questioned the validity of non-specific membrane binding as an explanation for increased biopotency. As a general phenomenon it should be effective also in the case of a C5a peptide and it is not, they argued [38]. The C5a molecule is related to C3a by sequence homology and a structurally conserved core [39], but C3a and C5a each interact with separate and unique receptors [38].

The observation of Ember et al. [38], however, does not lend itself to discriminating between the two concepts, because C5a activity is known not to be localized in the C-terminal sequence only as in C3a [40]. Furthermore in contrast to C3a the binding of C5a is not diffusion-limited probably because there are $N = 4000$ C5a receptors per guinea pig platelet [41].

Last not least the authors deduced the specific role of their appropriately positioned Trp pair from the existence of a hydrophobic patch on the surface of native C3a, consisting of Tyr^{59}, Ile^{60} and Leu^{63} [38]. A corresponding patch is displayed also on native C5a, made up of (Val^{56}), Val^{57}, Ala^{58} and Leu^{61}.

5. Conclusion

This study presents direct evidence that a hydrophobic anchor does enhance membrane binding, which correlates with a gain in biopotency. The concept of a secondary binding site can, of course, not be ruled out on the basis of the present results. Further investigations, e.g. a check on wether or not the peptides carrying two tryptophans at their N-terminus bind non-specifically to membranes, are required to rescue the secondary site from Occam's razor, it seems.

Acknowledgements

Thanks are due to Jürgen Stahl for the CD measurements and to Manfred Dewor for the amino acid analyses. We are grateful for the referees' comments and suggestions which led to considerable improvement of the article. This work was supported by a grant from the Bundesminister für Forschung und Technologie der Bundesrepublik Deutschland (Förderkennzeichen 01 VM 8901/4).

References

1 W.O. Weigle, M.G. Goodman, E.L. Morgan and T.E. Hugli, Springer Semin. Immunopathol. 6 (1983) 173.
2 T.E. Hugli, Springer Semin. Immunopathol. 7 (1984) 193.
3 T.E. Hugli, Complement 3 (1986) 111.
4 J. Köhl, M. Casaretto, M. Gier, G. Karwarth, C. Gietz, W. Bautsch, D. Saunders and D. Bitter-Suermann, Eur. J. Immunol. 20 (1990) 1463.
5 H.U. Gremlich, U.P. Fringeli and R. Schwyzer, Biochemistry 22 (1983) 4257.
6 R. Gerardy-Schahn, D. Ambrosius, M. Casaretto, J. Grötzinger, D. Saunders, A. Wollmer, D. Brandenburg and D. Bitter-Suermann, Biochem. J. 225 (1988) 209.
7 O.G. Berg, Makromol. Chem., Macromol. Symp. 17 (1988) 161.
8 S. Pind, A. Kuksis, J.J. Myher and L. Marai, Can. J. Biochem. Cell Biol. 62 (1984) 301.
9 D. Papahadjopoulos and H.K. Kimelberg, Phospholipid vesicles (liposomes) as models for biological membranes: their properties and interactions with cholesterol and proteins (Pergamon Press, New York, 1973).
10 E. Bucci and R.F. Steiner, Biophys. Chem. 30 (1988) 199.
11 E.J. Bolen and P.W. Holloway, Biochemistry 29 (1990) 9638.
12 R.A. Parente, L. Nadasdi, N.K. Subbarao and F.C. Szoka, Biochemistry 29 (1990) 8713.
13 L.R. McLean, K.A. Hagaman, T.J. Owen and J.L. Krstenansky, Biochemistry 30 (1991) 31.
14 R.M. Epand, A. Gawish, M. Iqbal, K.B. Gupta, C.H. Chen, J.P. Segrest and G.M. Anantharamaiah, J. Biol. Chem. 262 (1987) 9389.
15 D. Ambrosius, M. Casaretto, R. Gerardy-Schahn, D. Saunders, D. Brandenburg and H. Zahn, Biol. Chem. Hoppe-Seyler 370 (1989) 217.
16 H. Edelhoch, Biochemistry 6 (1967) 1948.
17 J. Brunner, P. Skrabal and H. Hauser, Biochim. Biophys. Acta 455 (1976) 322.
18 G.R. Bartlett, J. Biol. Chem. 234 (1959) 466.
19 G.C. Chen and J.T. Yang, Anal. Lett. 10 (1977) 1195.
20 H. Renscheidt, W. Straßburger, U. Glatter, A. Wollmer, G.G. Dodson and D.A. Mercola, Eur. J. Biochem. 142 (1984) 7.
21 S.W. Provencher and J. Glöckner, Biochemistry 20 (1981) 33.
22 D.R. James, D.R.M. Demmer, R.E. Verrall and R.P. Steer, Rev. Sci. Instrum. 54 (1983) 1121.
23 A.G. Szabo and D.M. Rayner, J. Am. Chem. Soc. 102 (1980) 554.
24 J.R. Lakowicz, Principles of fluorescence spectroscopy (Plenum Press, New York, 1983).
25 M.D. Barkley, A.A. Kowalczyk and L. Brand, J. Chem. Phys. 75 (1981) 3581.
26 R.E. Dale, L.A. Chen and L. Brand, J. Biol. Chem. 252 (1977) 7500.
27 C.I. Bashford, B. Chance, J.C. Smith and T. Yoshida, Biophys. J. 25 (1979) 63.
28 W.K. Surewicz and R.M. Epand, Biochemistry 23 (1984) 6072.
29 W.F. DeGrado and J.D. Lear, J. Am. Chem. Soc. 107 (1985) 7684.
30 L.K. Tamm and I. Bartoldus, FEBS Lett. 272 (1990) 29.
31 Y. Fukuoka and T.E. Hugli, J. Immunol. 140 (1988) 3496.
32 J.E. Gervasoni, D.H. Conrad, T.E. Hugli, L.B. Schwartz and S. Ruddy, J. Immunol. 136 (1986) 285.
33 J. Grötzinger, M. Engels, E. Jacoby, A. Wollmer and W. Straßburger, Prot. Eng. 4 (1991) 767.
34 R. Gerardy-Schahn, D. Ambrosius, D. Saunders, M. Casaretto, C. Mittler, G. Karwarth, S. Görgen and D. Bitter-Suermann, Eur. J. Immunol. 19 (1989) 1095.
35 R.P. Rand and V.A. Parsegian, Biochim. Biophys. Acta 988 (1989) 351.

36 V.V. Kumar, Proc. Natl. Acad. Sci. USA 88 (1991) 444.
37 J.A. Ember, N.L. Johansen and T.E. Hugli, Biochem. Soc. Trans. 18 (1990) 1154.
38 J.A. Ember, N.L. Johansen and T.E. Hugli, Biochemistry 30 (1991) 3603.
39 E.R.P. Zuiderweg, J. Henkin, K.W. Mollison, G.W. Carter and J. Greer, Proteins: Struc. Func. Genet. 3 (1988), 139.
40 K.W. Mollison, W. Mandecki, E.R.P. Zuiderweg, L. Fayer, T.A. Fey, R.A. Krause, R.G. Conway, L. Miller, R.P. Edalji, M.A. Shallcross, B. Lane, J.L. Fox, J. Greer and G.W. Carter, Proc. Natl. Acad. Sci. USA 86 (1989) 292.
41 T. Kretzschmar, K. Kahl, K. Rech, W. Bautsch, J. Köhl and D. Bitter-Suermann, Immunobiol. 183 (1991) 418.